Simultaneous retrieval of volcanic ash and SO_2 using MSG-SEVIRI measurements

A. J. Prata[1] and J. Kerkmann[2]

Received 6 November 2006; revised 1 December 2006; accepted 24 January 2007; published 10 March 2007.

[1] Volcanic ash and sulphur dioxide masses from the November 2005 eruption of Karthala volcano, Comoros Islands, are simultaneously retrieved using rapid-scan, multispectral infrared measurements from the Spin Enhanced Visible and Infrared Imager on board the Meteosat Second Generation geosynchronous satellite. Retrievals are made every 15 min, which show that the ash and SO_2 separate in the vertically sheared atmosphere producing a fast moving upper level ($\sim$12 km) SO_2 cloud, a slower moving middle level ($\sim$8 km) ash cloud and a boundary layer (<3 km) SO_2 plume. The total mass of fine ash is 0.1 ± 0.05 Tg (SiO_2), the upper level SO_2 mass is 0.19 ± 0.01 Tg (S) while the boundary layer SO_2 mass is 0.009 ± 0.01 Tg (S). These are the first simultaneous satellite measurements of ash and SO_2 from an erupting volcano and confirm previous ideas about vertical separation. We suggest care must be exercised when using SO_2 as a tracer for volcanic ash in aviation hazard warning systems. **Citation:** Prata, A. J., and J. Kerkmann (2007), Simultaneous retrieval of volcanic ash and SO_2 using MSG-SEVIRI measurements, *Geophys. Res. Lett.*, *34*, L05813, doi:10.1029/2006GL028691.

1. Introduction

[2] Erupting volcanoes can emit copious amounts of water vapour, CO_2, SO_2, and other gases as well as particulates, mostly in the form of fine (radii <10 μm) ash silicates. The largest gaseous components by volume are water vapour and CO_2. These gases are abundant in the background atmosphere and are of less interest than SO_2 and ash. Volcanic ash is recognized as a major hazard to aviation, principally because it can damage jet engines and cause them to shutdown [*Miller and Casadevall*, 2000]. Ash has been implicated in exacerbating respiratory ailments in children [*Forbes et al.*, 2003] and SO_2 is recognized as a health hazard causing inflammation and irritation of the eyes and respiratory tract [*Williams-Jones and Rymer*, 2000]. The residence time of volcanic ash in the atmosphere is short (hours to days), as most of the mass is contained at particle radii >10 μm, and these are rapidly removed from the atmosphere by gravity. Thus ash is not thought to play a role in causing climate effects, but its transport, dispersion and vertical placement are important for aviation and health hazard mitigation.

[3] The effects of SO_2 on air frames and engines is less well-known, but SO_2 is used as a tracer for volcanic clouds because both ash and SO_2 are erupted at the same time and can travel together in the atmosphere. SO_2 is of interest to climate scientists because in the troposphere it is a pollutant, can affect clouds and precipitation, while in the stratosphere SO_2 converts to H_2SO_4, and reflects solar radiation away from the earth causing surface cooling. For these reasons it is of some interest to identify, quantify and track the constituents of volcanic clouds.

[4] Satellites are well-suited to the task of identifying and tracking volcanic clouds [*Prata*, 1989; *Schneider et al.*, 1999; *Tupper et al.*, 2004]. Until recently, instruments on board polar orbiting and geosynchronous satellites played complementary roles–the high-spectral, low-temporal resolution polar sensors provide quantitative information [e.g., *Wen and Rose*, 1994; *Prata and Grant*, 2001], while the low-spectral, high-temporal resolution geosynchronous sensors have proved vital for tracking volcanic clouds [e.g., *Sawada*, 1987; *Tupper et al.*, 2007]. With the launch of the Meteosat Second Generation Spin Enhanced Visible and Infrared Imager (MSG-SEVIRI) into geosynchronous orbit it is now possible to obtain high-temporal and high-spectral resolution, quantitative estimates of volcanic constituents from space. We report the first simultaneous measurements of volcanic ash and SO_2 using five infrared channels of the MSG-SEVIRI centred at, 6.2, 7.3, 8.5, 11 and 12 μm. The paper is brief: we describe the volcanic setting and eruption information, some details of the MSG-SEVIRI, discuss the retrieval scheme and make some general conclusions concerning the vertical separation and movement of the volcanic constituents.

2. Karthala Volcano Eruption

[5] The Karthala volcano forms most of the land-mass of Grande Comoro (also called Ngazidja), the main island of the Union of the Comoros. It is situated at 11.75°S and 43.38°E in the Indian Ocean (see Figure 1) and is one of the largest active volcanoes in the world. Over the last two hundred years, it has erupted every eleven years on average. The 24–25 November 2005 eruption is described in the Smithsonian's Bulletin of Global Volcanism Network report of November 2005 (Smithsonian Institution, 2005) and January 2006 report (Smithsonian Institution, 2006). According to the Karthala National Observatory, the eruption on 24 November 2005 was probably phreatic in its initial phase, that is, it was caused by vaporization of ground water in contact with a shallow magma body underneath the crater. In these cases water vapour forms immediately, breaking the surrounding rocks and throwing them in the spaces close to the caldera. The eruption which started on the 24 November, at around 16:00 LT (LT = local time = UTC + 2), entered the second phase (the magmatic phase), in the afternoon of 25 November, with the appear-

[1]Norwegian Institute for Air Research (NILU), Kjeller, Norway.
[2]European Organisation for the Exploitation of Meteorological Satellites (EUMETSAT), Darmstadt, Germany.

0094-8276/07/2006GL028691$05.00

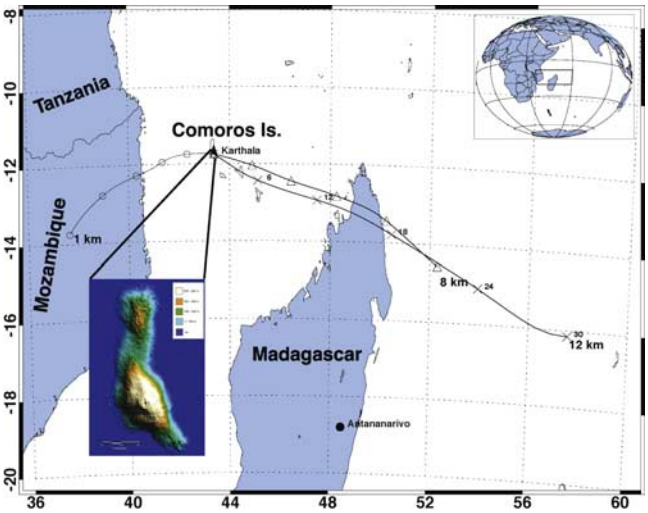

Figure 1. Map of the Comoros islands. Also shown are three HYSPLIT trajectories at 3, 8 and 12 km that closely match the positions of the low-level SO_2 plume, the middle-level ash cloud and the high-level SO_2 cloud observed in SEVIRI data.

ance of a red cloud above the caldera, caused by the formation of a lava lake. In the capital, Moroni, ash fell from 02:00 LT on 25 November, resulting in almost no visibility. Reports (see Smithsonian Institution, 2006) suggest that by 09:00 LT the sky was darkened by ash-fall; much of it was carried to the south-west area of the island. Ash deposits in the streets were in some places up to 10 cm thick–see the photographs published on-line by Smithsonian Institution (2006). The eruption had the effect of killing at least one infant, infiltrating homes, shops and offices and contaminating water in cisterns during the height of the dry season. Cistern water supplies for about 120,000 residents mainly from rural villages near the volcano had been contaminated by the ash. The ash-fall also raised fears of respiratory ailments. As reported by the head of the Meteorological Department of the international airport of Karthala, there were some international flights (Air Tanzania, Air Austral) and several local flights cancelled, during 26–27 November. Even after the airport traffic was restored late on the 27th, a local flight coming towards Moroni from Madagascar had to return to its airport of departure, because it encountered an ash cloud on its way to Moroni. Karthala volcano's eruption ended after 14 days on 8 December 2005.

[6] Our study concentrates on the aviation critical period from the beginning of the magmatic phase of the eruption up to 48 hours afterwards. It is well documented that most serious (engine damage) aviation incidents occur within the first few hours of an eruption.

3. MSG-SEVIRI

[7] The Meteosat Second Generation (MSG) platform is Europe's principal operational weather satellite. It was launched on 28 August 2002 and became fully operational on 21 January 2004 supporting 17 European member states. MSG is a geosynchronous satellite, orbiting the earth at a height of 42,000 km with a period of 24 hours and a nadir point at approximately 3°W over the equator. The Spin Enhanced Visible and Infra-Red Instrument (SEVIRI) is spin-stabilised and obtains image data by rotating at 100 rpm about an axis oriented parallel to the north-south axis of the earth, and stepping a scan mirror to build up an image. The resulting image spans a field of view of approximately 70 degrees at the earth's surface. SEVIRI is a heritage instrument– its specification has been influenced by previous experience with earlier instruments. The 12 channels spanning the visible to infrared regions have been carefully selected and optimized to provide weather information and hence are not ideal for retrieving volcanic cloud information. The infrared channels are sampled at 3 km intervals, but the instantaneous field of view is ~4.8 km. Further detail on MSG and SEVIRI can be obtained from the downloadable documents located at http://www.eumetsat.int.

4. Retrieval Schemes

4.1. Volcanic Ash

[8] Volcanic ash has become a generic term used to describe the particulate emissions from volcanic eruptions. The major constituent of volcanic ash is SiO_2 (silicate) which occurs in varying amounts from 50% upwards. Measurements of the Mt St Helens ash-fall deposits showed that they contained between 50–69% SiO_2 [*Mullineaux and Crandell*, 1981]. The remaining components of volcanic ash are minerals: Fe, Mg and Al, are common. Fine ash particles typically have equivalent radii of 1–10 μm and are closest to spheroidal in shape, but often contain asperites and aggregations of smaller particles. Identification and quantification of volcanic ash using infrared remote sensing relies on assumptions concerning the silicate content (refractive indices), particle size distribution, cloud opacity, thermal contrast (temperature difference between the ash cloud and background), and to a lesser extent the particle shapes. These factors have been explored in detail by *Wen and Rose* [1994] and *Prata and Grant* [2001].

4.2. Mass

[9] *Prata and Grant* [2001] describe an ash mass retrieval scheme using two infrared channels and a microphysical model of an ash cloud. The input information consists of assumed values for the refractive indices of ash averaged over the infrared channel bandwidths, a particle size distribution model (a modified-γ distribution is used [e.g., *Press et al.*, 1986]), spherical particles, homogeneous ash cloud, isotropic radiation field and neglect of absorption, transmission and scattering of radiation in the atmosphere above the cloud layer. Computation of the radiation field emerging upwards from the ash cloud layer at up to 16 scattering angles, together with the satellite measurements, provides a set of data that can be inverted to deliver mean particle size and optical depth. These parameters are related to the mass loading (kg m^{-3}) by,

$$M = \frac{4\pi\rho}{3}\int_o^\infty r^3 n(r)dr, \quad (1)$$

where $\boldsymbol{\rho}$ is the density of the ash and $\mathbf{n(r)}$ is the size distribution. The total mass can be calculated by multiplying

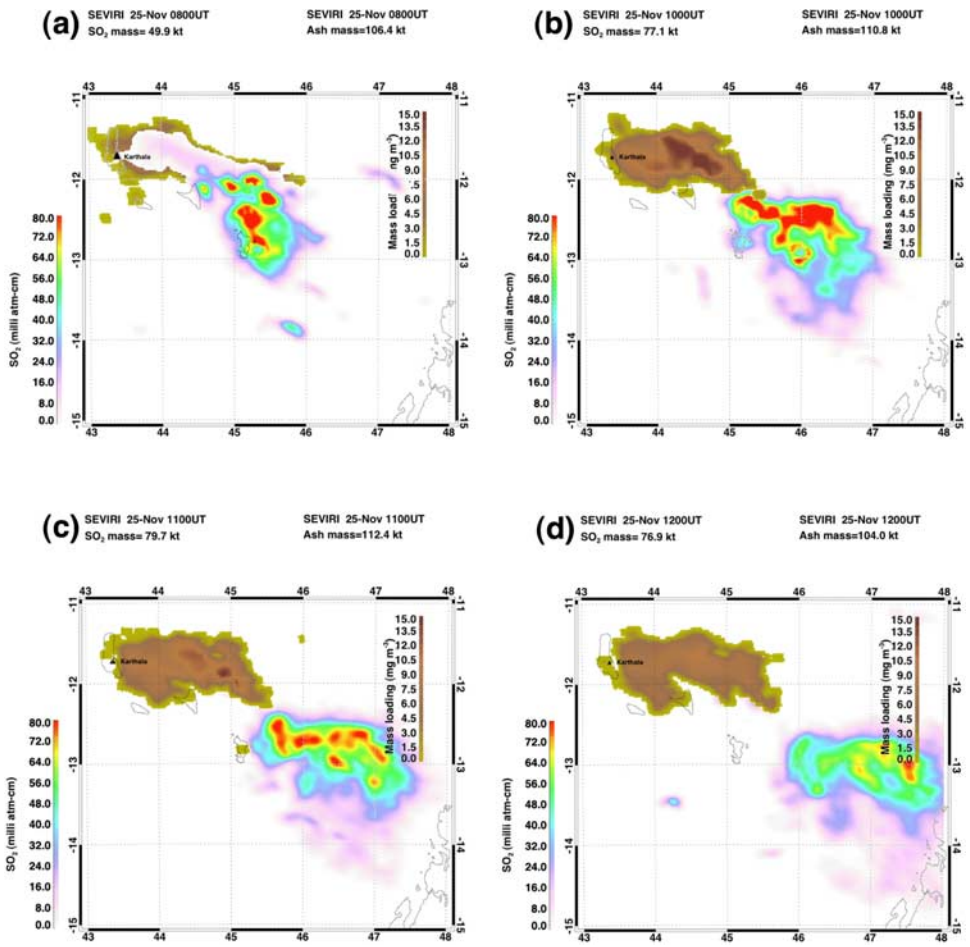

Figure 2. SEVIRI ash and SO_2 retrievals at four different times on 25 November, 2005.

M by the volume of a pixel (geometric thickness multiplied by the area of a pixel). Sensitivity analyses by *Wen and Rose* [1994] suggest mass loading errors of ~40–50%.

4.3. SO_2 Retrieval

[10] Sulphur dioxide is retrieved from SEVIRI data using channels at 7.3 μm and 8.6 μm. SO_2 absorbs strongly in both of these regions. The strong absorption at 7.3 μm is affected by water vapour and thus this channel is used to retrieve SO_2 that is high (>3 km) in the atmosphere, and hence above most of the water vapour. The 8.6 μm channel lies in a relatively transparent region and can be used to retrieve boundary layer SO_2. *Prata et al.* [2003] describe a retrieval scheme using the TOVS/HIRS 7.3 μm channel, while *Watson et al.* [2004] and *Realmuto et al.* [1994] describe methods for retrieving SO_2 from 8.6 μm radiation from MODIS and ASTER data, respectively. In applying these retrieval schemes to SEVIRI data, the appropriate channel response functions have been used in off-line radiative transfer calculations to obtain the required parameters. In the case of the 7.3 μm channel, an exponential sum-fit procedure [see *Prata et al.*, 2003] is used to relate transmittance to SO_2 column amount, while for the 8.6 μm retrieval a quadratic fit between SO_2 and brightness temperature difference is used, based on parameters determined from Modtran 3 [*Berk et al.*, 1989] simulations. In summary 'high-level' SO_2 is determined from,

$$t_s = \sum_{i=1}^{n} a_i \exp(-k_i u), \tag{2}$$

where t_s is the transmittance (related to the 7.3 μm brightness temperature), $\mathbf{u}$ is absorber amount, and $\mathbf{a}_i$, $\mathbf{k}_i$ are coefficients. Low-level SO_2 from the 8.6 μm channel is determined from,

$$u = b_o + b_1 \Delta T + b_2 \Delta T^2 \tag{3}$$

where $\mathbf{b}_i$, i = 0, 2, are coefficients, and, $\Delta T = T_{8.6} - T_{12}$ · $T_{8.6}$ and T_{12} are top-of-atmosphere brightness temperatures at 8.6 μm and 12 μm, respectively.

[11] We emphasize here that neither of these SEVIRI retrieval schemes have been properly validated against independent measurements. Based on an error budget for the TOVS/HIRS SO_2 retrieval scheme [*Prata et al.*, 2003], a conservative error for SEVIRI is ±10 D.U. on a single pixel basis. This gives a mass loading retrieval error of approximately ±0.01 Tg(S), for the SO_2 clouds discussed here.

5. Separation of the Dispersing Volcanic Cloud

[12] Figure 2 shows a series of four images of the low-level SO_2 plume, medium-level ash cloud and high-level SO_2

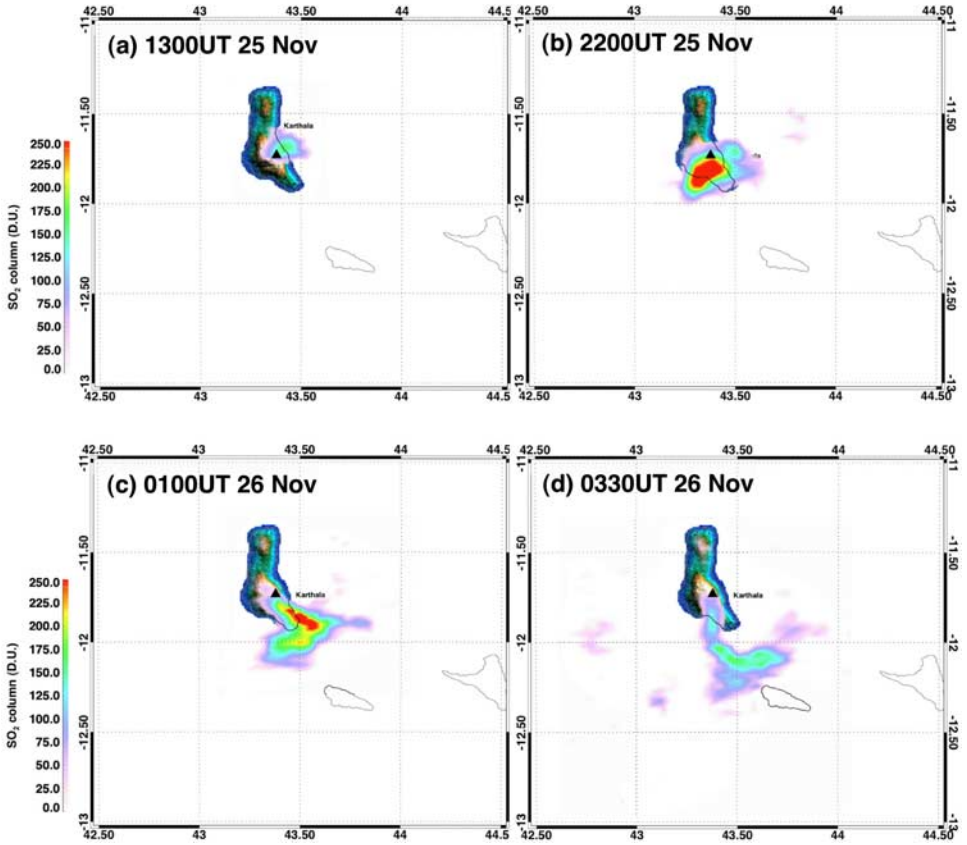

Figure 3. SEVIRI low-level SO_2 retrievals at four different times during 25–26 November 2005.

cloud determined from SEVIRI data. HYSPLIT [*Draxler and Rolph*, 2003] trajectories for three levels in the atmosphere (3 km, 8 km and 12 km) are shown in Figure 1. The low-level plume has a westward component, but also travels south and later (25 November) moves eastwards. This plume is largely trapped in the boundary layer winds and is affected by local topographic and land-sea breeze circulations. The middle-level ash layer travels predominantly eastwards, although as discussed earlier, some of the ash fell directly onto Grand Comoros. The ash cloud travelled towards northern Madagascar, crossing the island and entering the Indian ocean before becoming too dispersed to be detectable by SEVIRI. The high-level SO_2 cloud also travelled eastwards, just south of the ash cloud but at a quicker pace. A rawinsonde ascent obtained at Antananarivo (see Figure 1 for location) at 23:00 UT on 24 November shows that winds above 17 km (55,000 feet) changed from westerly to easterly, reaching 10–15 ms^{-1} between 18–24 km. The tropopause level on this ascent was located at ~15 km, so it is concluded that the ash and SO_2 did not penetrate the stratosphere. Winds increase in speed from ~9 ms^{-1} to ~15 ms^{-1} between 7.6 km and 12.3 km. The wind speed difference leads to ~520 km of horizontal separation after 24 hours, between the ash and high-level SO_2 cloud, with the SO_2 cloud leading. The separation due to vertical shear is clearly evident in the panels of Figure 2. This observation is of significance to the aviation industry because different airways are affected by different hazards. In the case of an SO_2 encounter it is still unknown how serious the effects may be. Knowledge of the main constituents in a volcanic cloud during an encounter will help diagnose damage and will provide information for post-encounter maintenance.

[13] The low-level plume observed by SEVIRI is illustrated in the four panels of Figure 3. The total SO_2 loadings are not large: typically the mass loading in each image is 1–10 kt. The estimated SO_2 emission rate is ~60 kg s^{-1}, with peak rates of ~260 kg s^{-1}, and the integrated mass loading for the 48 hour period starting at 12:00 UT on 24 November is 0.009 Tg (SO_2). Ozone Monitoring Instrument (OMI) [*Krotkov et al.*, 2006] SO_2 measurements on 25–28 November show extensive but low (<6 D.U.) amounts of SO_2 observed in the vicinity of the Comoros (Simon Carn, private communication).

6. Discussion

[14] The high temporal resolution of the measurements from SEVIRI, together with good spatial resolution and spectral imaging capability has permitted the first simultaneous retrievals of volcanic constituents from satellite. Figure 4 shows the time-series of measurements from the start of the eruption on 24 November to midday on 26 November, for three parts of the volcanic cloud identified from the data: a low-level SO_2 plume (blue bars), a middle-level ash cloud (red line) and a high-level SO_2 cloud (black line).

[15] The low-level plume has 4–5 noticeable peaks; the largest of these occurs around 0100 UT on 26 November during a period when the ash and high-level SO_2 amounts are low. The maximum ash mass is observed during 08:00–12:00 UT on 25 November, when ash-fall in Moroni was

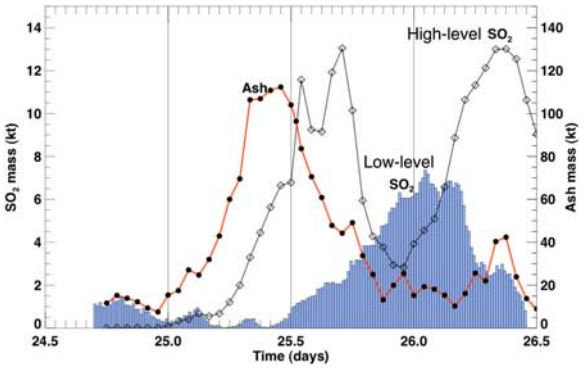

Figure 4. Time-series of ash and SO_2 masses during 24–26 November, 2005. The low-level SO_2 plume is shown as blue bars, the middle-level ash cloud as a red line with black dots and the high-level SO_2 cloud as a gray line and diamonds.

reported as severe. A second ash maximum occurs on the following day at around 09:00 UT, presumably associated with an earlier eruption. The first ash maximum precedes the high-level SO_2 maximum by about 6 hours, while the second maximum is coincident with a second SO_2 maximum. The low-level plume behaviour may reflect small eruptive activity or passive degassing and its relationship to the higher level eruptive products is probably not significant. The temporal relationship between the higher level ash and SO_2 suggests that initially, the SO_2 may be trapped by the ash or possibly ice and is not fully revealed until re-evaporation into the gas phase has occurred. *Kärcher and Basko* [2004] describe a model for the process of gas trapping by ice particles and gas release by evaporation and *Rose et al.* [1995] have observed ice in volcanic eruption clouds. The amount of ice in this eruption cloud has not been determined, but the cloud is well above the freezing level and the SEVIRI data suggest that ice is present.

[16] The low-level cloud was mostly SO_2, and together with fall-out from the middle-level ash cloud and low-level ash emissions, caused significant disruption to infrastructure and health hazards on Grand Comoros, during the last week of November 2005. SEVIRI and OMI data analyses indicate that the low-level plume did not reach Mozambique or Tanzania, but the middle-level ash and high-level SO_2 travelled to Madagascar and further into the Indian ocean. A false-colour movie-loop, at 15-min time intervals can be viewed in the auxiliary materials[1]. The movie-loop shows that when the middle-level ash reached northern Madagascar around 19:00 UT on 25 November, convection there was suppressed. Once the ash had passed over Madagascar convective cloud formation there halts, while further south the clouds continue to build up. Ash particles can reduce the effective size of cloud particles [*Tupper et al.*, 2005], and hence suppress convective activity and reduce precipitation [e.g., *Rudich et al.*, 2002].

[17] The low-level plume remained near the Comoros, but it is likely this plume was largely SO_2 and because it was low level it would not have caused major disruption to intercontinental and trans-Indian ocean air-traffic, but may have posed a health hazard. The vertical shearing of the wind caused much of the ash and SO_2 to be quickly removed from the vicinity of the Comoros, with the SO_2 cloud leading the ash cloud and separating from it. Both clouds moved into the Indian ocean, east of Madagascar intersecting flight routes and posing a threat to aviation. Identification of the constituents and movement of drifting volcanic clouds can be improved by using SO_2 and ash retrievals from operational satellites and providing this information in a timely manner to aviation authorities.

[1]Auxiliary materials are available in the HTML. doi:10.1029/2006GL028691.

References

Berk, A., L. S. Bernstein, and D. C. Robertson (1989), MODTRAN: A moderate resolution model for LOWTRAN 7, *AFGL-TR-89-0122*, U. S. Air Force Phillips Lab., Nascom Air Force Base, Mass.

Draxler, R. R., and G. D. Rolph (2003), HYSPLIT (HYbrid Single-Particle Lagrangian Integrated Trajectory) Model access, http://www.arl.noaa.gov/ready/hysplit4.html, Air Resour. Lab., NOAA, Silver Spring, Md.

Forbes, L., D. Jarvis, J. Potts, and P. J. Baxter (2003), Volcanic ash and respiratory symptoms in children on the island of Montserrat, British West Indies, *Occup. Environ. Med.*, *60*, 207–211.

Kärcher, B., and M. M. Basko (2004), Trapping of trace gases in growing ice crystals, *J. Geophys. Res.*, *109*, D22204, doi:10.1029/2004JD005254.

Krotkov, N. A., S. A. Carn, A. J. Krueger, P. K. Bhartia, and K. Yang (2006), Band residual difference algorithm for retrieval of SO_2 from the Aura Ozone Monitoring Instrument (OMI), *IEEE Trans. Geosci. Remote Sens.*, *44*(5), 1259–1266.

Miller, T. P., and T. J. Casadevall (2000), Volcanic ash hazards to aviation, in *Encyclopedia of Volcanoes*, edited by H. Sigurdsson, pp. 915–930, Elsevier, New York.

Mullineaux, D. R., and D. R. Crandell (1981), The eruptive history of Mount St. Helens, in *The 1980 Eruptions of Mount St. Helens, Washington*, *Geol. Surv. Prof. Pap.*, *1250*, 3–15.

Prata, A. J. (1989), Radiative transfer calculations for volcanic ash clouds, *Geophys. Res. Lett.*, *16*, 1293–1296.

Prata, A. J., and I. F. Grant (2001), Retrieval of microphysical and morphological properties of volcanic ash plumes from satellite data: Application to Mt. Ruapehu, New Zealand., *Q. J. R. Meteorol. Soc.*, *127*(576B), 2153–2179.

Prata, A. J., W. I. Rose, S. Self, and D. M. O'Brien (2003), Global, long-term sulphur dioxide measurements from TOVS data: A new tool for studying explosive volcanism and climate, in *Volcanism and the Earth's Atmosphere*, *Geophys. Monogr. Ser.*, vol. 139, edited by A. Robock and C. Oppenheimer, pp. 75–92, AGU, Washington, D. C.

Press, W. H., B. P. Flannery, S. A. Teukolsky, and W. T. Vetterling (1986), *Numerical Recipes*, 818 pp., Cambridge Univ. Press, New York.

Realmuto, V. J., M. J. Abrams, M. F. Buongiorno, and D. C. Pieri (1994), The use of multispectral thermal infrared image data to estimate the sulfur-dioxide flux from volcanoes: A case study from Mount Etna, Sicily, July 29, 1986, *J. Geophys. Res.*, *99*(B1), 481–488.

Rose, W. I., D. J. Delene, D. J. Schneider, G. J. S. Bluth, A. J. Krueger, I. Sprod, C. McKee, H. L. Davies, and G. G. J. Ernst (1995), Ice in the 1994 Rabaul eruption cloud: Implications for volcano hazard and atmospheric effects, *Nature*, *375*, 477–479.

Rudich, Y., O. Khersonsky, and D. Rosenfeld (2002), Treating clouds with a grain of salt, *Geophys. Res. Lett.*, *29*(22), 2060, doi:10.1029/2002GL016055.

Sawada, Y. (1987), Study on analysis of volcanic eruptions based on eruption cloud image data obtained by the Geostationary Meteorological Satellite (GMS), *Tech. Rep. 22*, 335 pp., Meteorol. Res. Inst., Tsukuba, Japan.

Schneider, D. J., W. I. Rose, L. R. Coke, G. J. S. Bluth, I. Sprod, and A. J. Krueger (1999), Early evolution of a stratospheric volcanic eruption cloud as observed with TOMS and AVHRR, *J. Geophys. Res.*, *104*(D4), 4037–4050.

Smithsonian Institution (2005), Karthala, *Bull. Glob. Volcanism Netw.* *30*(11), 2–4.

Smithsonian Institution (2006), Karthala, *Bull. Glob. Volcanism Netw.* *31*(1), 2–4.

Tupper, A., S. A. Carn, J. Davey, Y. Kamada, R. J. Potts, A. J. Prata, and M. Tokuno (2004), An evaluation of volcanic cloud detection techniques during recent significant eruptions in the western 'Ring of Fire,' *Remote Sens. Environ.*, *91*, 27–46.

Tupper, A., J. S. Oswalt, and D. Rosenfeld (2005), Satellite and radar analysis of the volcanic-cumulonimbi at Mount Pinatubo, Philippines, 1991, *J. Geophys. Res.*, *110*, D09204, doi:10.1029/2004JD005499.

Tupper, A., I. Itakarai, M. Richards, A. J. Prata, S. A. Carn, and D. Rosenfeld (2007), Facing the challenges of the International Airways Volcano Watch: The 2004/05 eruptions of Manam, Papua New Guinea, *Weather Forecast*., in press.

Watson, I. M., V. J. Realmuto, W. I. Rose, A. J. Prata, G. J. S. Bluth, Y. Gu, C. E. Bader, and T. Yu (2004), Thermal infrared remote sensing of volcanic emissions using the moderate resolution imaging spectroradiometer, *J. Volcanol. Geotherm. Res.*, *135*, 75–89.

Wen, S., and W. I. Rose (1994), Retrieval of sizes and total masses of particles in volcanic clouds using AVHRR channels 4 and 5, *J. Geophys. Res.*, *99*(D3), 5421–5431.

Williams-Jones, G., and H. Rymer (2000), Hazards of volcanic gases, in *Encyclopedia of Volcanoes*, edited by H. Sigurdsson, pp. 997–1004, Elsevier, New York.

J. Kerkmann, European Organisation for the Exploitation of Meteorological Satellites (EUMETSAT), Am Kavalleriesand 31, D-64295 Darmstadt, Germany.

A. J. Prata, Norwegian Institute for Air Research (NILU), P.O. Box 100, N-2027 Kjeller, Norway. (fred.prata@nilu.no)